was fully characterized.[9,10] Precedent could be cited for expecting dehydrohalogenation of **2c** by hindered base,[11] but there are other precedents for boron-assisted displacements by highly hindered nucleophiles.[8,11,12]

Desilylation of **3c** with methanol gave impure ethylene glycol 1-amino-2-phenylethaneboronate, $PhCH_2CH(NH_2)BO_2C_2H_4$, unstable to distillation.[13] Its isolation was bypassed by treating **3c** with acetic anhydride and acetic acid, which yielded 86% ethylene glycol 1-acetamido-2-phenylethaneboronate (**4c**),[10,14] a distillable solid, too water soluble to be extracted into ether.

The directed chiral synthesis of pinanediol α-chloro boronic esters[15] was used to make the separate enantiomers of 1-acetamido-2-phenylethaneboronic acid (**5a** and **5b**). Optically pure (+)-pinanediol benzylboronate (**1a**)[10,16] was homologated with (dichloromethyl)lithium[15] to **2a**, which was treated in situ with lithiohexamethyldisilazane followed by acetic anhydride and acetic acid to yield (+)-pinanediol (*R*)-1-acetamido-2-phenylethaneboronate (**4a**), 63% isolated by chromatography, recrystallized from dichloromethane to constant rotation.[10,17] Destructive cleavage of the pinanediol ester with boron trichloride[15] yielded (*R*)-1-acetamido-2-phenylethaneboronic acid (**5a**), which was characterized as its reversibly formed boronic anhydride.[10,18] The *S* enantiomers were similarly prepared.[19]

The affinity of chymotrypsin for the *R* and *S* isomers of 1-acetamido-2-phenylethaneboronic acid (**5a** and **5b**) was determined by examining the effects of these compounds on the rates of hydrolysis of methyl hippurate.[1] The reciprocal plots of initial velocity against substrate concentration given in Figure 1 show the pattern characteristic of competitive inhibition.[20] The competitive nature of the inhibition indicates that the compounds bind at the active site. The values of the dissociation constants, which were obtained from the data by standard equations,[20,21] are 2.1×10^{-6} M for the *R* isomer (**5a**) and 5.3×10^{-5} M (or greater if optical purity < 100%) for the *S* isomer (**5b**). The dissociation constant for 2-phenylethaneboronic acid, which lacks the acetamido substituent, was previously found to be 4×10^{-5} M.[1] The fact that (*R*)-1-acetamido-2-phenylethaneboronic acid (**5a**) binds the most tightly agrees with expectations[1] based upon the properties of the corresponding carbon compounds: L-phenylalanine derivatives are hydrolyzed by chymotrypsin much more rapidly than are 3-phenylpropionic acid and D-phenylalanine derivatives, although the three classes bind to the enzyme with about the same strength.[7,22] The affinity of chymotrypsin for the (*R*)-boronic acid **5a** is about 14 000 times greater than that for *N*-acetyl-L-phenylalanine amide.[7]

Acknowledgment. D.S.M. thanks the National Institutes of Health for financial support (Grant GM-27109).[24]

(9) One equivalent of **2c** was added to $LiN(SiMe_3)_2$ in THF at −78 °C, the mixture kept overnight at 20 °C, and the product distilled from LiCl; bp 103–104 °C (0.03 torr), ^1H NMR ($CDCl_3$) δ 0.15 (s, 18, $SiCH_3$), 2.95 (m, 3, CH_2CH), 4.23 (s, 4, OCH_2), 7.40 (s, 5, C_6H_5).

(10) Satisfactory analyses (±0.3%) were obtained for all elements except oxygen.

(11) (a) Matteson, D. S.; Mah, R. W. H. *J. Org. Chem.* **1963**, *28*, 2174–2176. (b) Reaction of $PhCH_2CHIBO_2C_2(CH_3)_4$[6d] with $LiN(COCH_3)_2$ yielded $PhCH{=}CHBO_2C_2(CH_3)_4$. Matteson, D. S., unpublished.

(12) Brown, H. C.; De Lue, N. R.; Yamamoto, Y.; Maruyama, K.; Kasahara, T.; Murahashi, S.; Sonoda, A. *J. Org. Chem.* **1977**, *42*, 4088–4092.

(13) Treatment of **3c** with methanol at 0 °C followed by vacuum concentration and washing the residue with ether gave impure $PhCH_2CH(NH_2)BO_2C_2H_4$, mp 143–149 °C. ^1H NMR in D_2O/CF_3CO_2H showed a single CH_2CH peak at δ 3.1, distinctly different from the multiplet of added $PhCH_2CH_2NH_2$.

(14) A THF solution of **3c** at −78 °C was treated with 3 equiv of acetic anhydride and 1 equiv of acetic acid, kept at 20 °C for 15 h, and distilled; bp 143–145 °C (0.03 torr), resublimed, mp 128 °C; H NMR ($CDCl_3$) δ 2.04 (s, 3, $COCH_3$), 2.75 (m, 3, CH_2CH, resolved to doublet and triplet by Eu(fod)$_3$), 3.90 (s, 4, OCH_2), 7.40 (s, 5, C_6H_5), 7.10, concentration dependent (br s, 1, N*H*); ^{13}C NMR consistent with assigned structure.

(15) Matteson, D. S.; Ray, R. *J. Am. Chem. Soc.* **1980**, *102*, 7590–7591.

(16) Bp 108 °C (0.1 torr); $[\alpha]^{22}_D$ + 31.30° (*c* 18, toluene); ^1H NMR consistent with assigned structure.

(17) Eluted from silica gel with ether, recrystallized three times (CH_2Cl_2), mp 185–186 °C; $[\alpha]^{20}_D$ −82.4° (*c* 3–5, $CHCl_3$); ^1H NMR ($CDCl_3$) δ 0.8–2.5 (m, 18, pinane + $COCH_3$), 2.9 (m, 3, $CHCH_2$), 4.32 (m, 1, OCH), 7.36 (s, 5, C_6H_5); ^{13}C NMR consistent with assigned structure.

(18) The mixture was concentrated under vacuum and the residue was washed with ether, treated with methanol, concentrated, dissolved in water, and neutralized with Dowex 1-X8 ion exchange resin bicarbonate, concentrated, and crystallized from THF/water, 80–85%; $[\alpha]^{22}_D$ −196° (*c* 0.6, H_2O) for the boronic anhydride; ^1H NMR (CD_3OD) δ 2.20 (s, 3, $COCH_3$), 2.82 (m, 3, CH_2CH), 5.2 (s, ~2.5, OH + NH), 7.40 (s, 5, C_6H_5); ^{13}C NMR (D_2O) δ 176.36 ($COCH_3$); 140.57, 128.68 (2), 128.55 (2), 128.55 (2), 126.21 (C_6H_5); 49.56 (br, CHNB); 36.18 ($PhCH_2$); 16.11 ($COCH_3$). Potentiometric titration showed 1 mol of boronic acid, pK = 8.85.

(19) **4b**: $[\alpha]^{22}_D$ + 83.3° (*c* 3, $CHCl_3$). **5b**: $[\alpha]^{22}_D$ + 195° (*c* 0.7, H_2O) for sample of composition $C_{10}H_{12}BNO_2{\cdot}0.25H_2O$.[10]

(20) Dixon, M.; Webb, E. C. "Enzymes", 3rd ed.; Academic Press: New York, 1979; pp 332–381.

(21) In the case of the *R* isomer, eq VIII.89 of ref 20 was used, since significant fractions of the added inhibitor (20–35%) are bound to the enzyme.

(22) Ingles, D. W.; Knowles, J. R. *Biochem. J.* **1968**, *108*, 561–569.

(23) Kezdy, F. J.; Clement, G. E.; Bender, M. L. *J. Am. Chem. Soc.* **1964**, *86*, 3690–3696.

(24) After completing this work, we learned of the interest of Dr. Manfred Philipp in boronic acids as enzyme inhibitors and sent him a sample of **5a**. He has found **5a** to be a competitive inhibitor of subtilisin, k_i(lim) = 1.7×10^{-6} M. We thank Dr. Philipp for informing us of these results: Philipp, M.; Sreenivasulu, M., manuscript submitted for publication.

Flavoprotein Monooxygenases: A Chemical Model

John W. Frost and William H. Rastetter*[1]

Department of Chemistry
Massachusetts Institute of Technology
Cambridge, Massachusetts 02139
Received May 4, 1981

Among the metabolic functions of the flavin-dependent monooxygenases[2] is the ortho hydroxylation of phenolic substrates such as salicylate and *p*-hydroxybenzoate. The unique position of the flavoproteins among biological hydroxylases follows from the reactivity of the metal-free, reduced isoalloxazine (dihydroflavin) nucleus with molecular oxygen. Evidence points to a subsequently formed 4α-hydroperoxide (**10**, Scheme II) as the molecular species responsible for, or leading to, flavin monooxygenase activity.[3] Herein we present a chemical model which suggests a flavin-based nitroxyl radical as the hydroxylating agent in the flavin monooxygenase ortho hydroxylation of phenolic substrates. Possible in vivo routes from the putative 4α-(hydroperoxy)flavin to an N^5-nitroxyl radical are discussed.

The flavin model work of Bruice et al.[4,5] has demonstrated the extremely facile oxidation of sulfides and amines and the dioxygenation of phenolate anions by 5-ethyl-3-methyl-4α-(hydroxyperoxy)lumiflavin. However, no flavin *mono*oxygenase model system has adequately explained flavin-mediated hydroxylation of phenols.[6] Our earlier work[7] with flavin N^5-oxide **1a** (Scheme I) showed the photolytic transfer of the N^5-oxygen

(1) Alfred P. Sloan Fellow, 1980–1982.

(2) (a) Walsh, C. *Acc. Chem. Res.* **1980**, *13*, 148. (b) Massey, V.; Hemmerich, P. *Enzymes, 3rd Ed.* **1976**, *12*, 191. (c) Hemmerich, P. *Fortschr. Chem. Org. Naturst.* **1976**, *33*, 451. (d) Dagley, S. In "Essays in Biochemistry", Campbell, P. N., Aldridge, W. N., Eds.; Academic Press: New York, 1975; Vol. 11, p 81. (e) Flashner, M. S.; Massey, V. In "Molecular Mechanisms of Oxygen Activation", Hayaishi, O., Ed.; Academic Press: New York, 1974; p 245.

(3) (a) Spector, T.; Massey, V. *J. Biol. Chem.* **1972**, *247*, 7123. (b) Strickland, S.; Massey, V. *Ibid.* **1973**, *248*, 2953. (c) Entsch, B.; Massey, V.; Ballou, D. P. *Biochem. Biophys. Res. Commun.* **1974**, *57*, 1018. (d) Entsch, B.; Ballou, D. P.; Massey, V. *J. Biol. Chem.* **1976**, *251*, 2550. (e) Kemal, C.; Bruice, T. C. *Proc. Natl. Acad. Sci. U.S.A.* **1976**, *73*, 995. (f) Presswood, R.; Kamin, H. In "Flavins and Flavoproteins, Proceedings of the Fifth International Symposium", Singer, T. P., Ed.; Elsevier: New York, 1976; p 145. (g) Ghisha, S.; Entsch, B.; Massey, V.; Husein, M. *Eur. J. Biochem.* **1977**, *76*, 139.

(4) (a) Ball, S.; Bruice, T. C. *J. Am. Chem. Soc.* **1979**, *101*, 4017. (b) *Ibid.* **1980**, *102*, 6498.

(5) (a) Kemal, C.; Bruice, T. C. *J. Am. Chem. Soc.* **1979**, *101*, 1635. (b) Bruice, T. C.; Muto, S. *Ibid.* **1980**, *102*, 4472. (c) Iwata, M.; Bruice, T. C.; Carrell, H. L.; Glusker, J. P. *Ibid.* **1980**, *102*, 5036.

(6) Bruice has suggested that flavoprotein monooxygenase activity may be explained by initial dioxygenation of phenolic substrates.[5a]

(7) Rastetter, W. H.; Gadek, T. R.; Tane, J. R.; Frost, J. W. *J. Am. Chem. Soc.* **1979**, *101*, 2228.

0002-7863/81/1503-5242$01.25/0

Scheme I

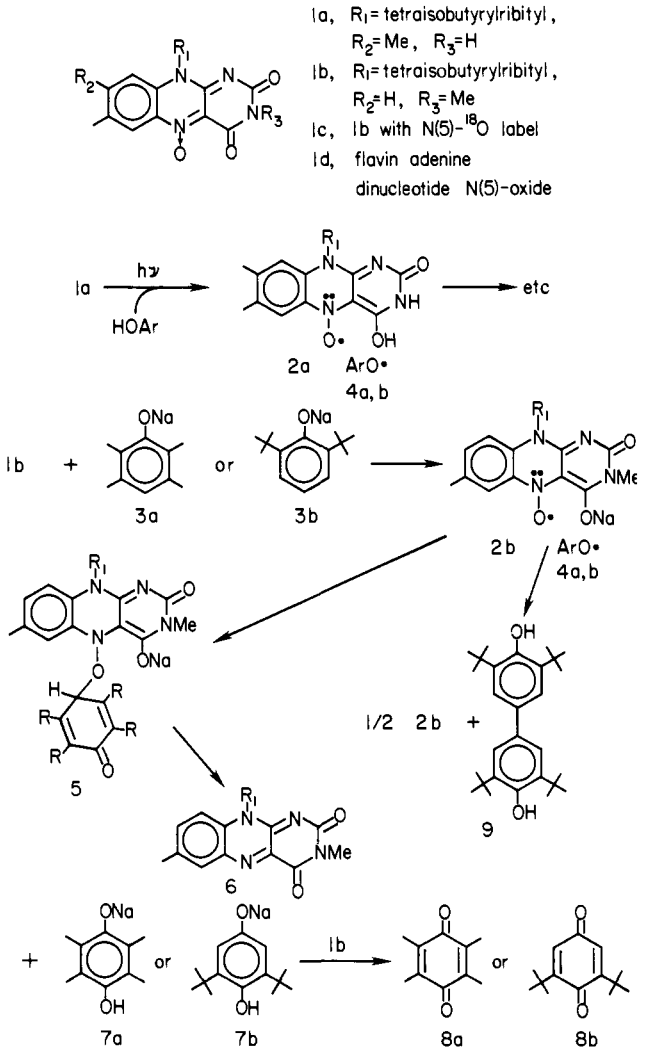

atom to phenols, ultimately producing benzoquinones. The species likely responsible for the oxygen transfer is N^5-nitroxyl radical **2a** or a tautomer. Nonetheless, the need for photoactivation of the flavin N^5-oxide clouded the relevance of our model system to the in vivo, ground-state flavin mediated phenol hydroxylations.

In principle, a flavin N^5-nitroxyl radical anion (see **2b**, Scheme I) could be generated nonphotochemically by electron transfer from phenolic substrate to flavin N^5-oxide. However, the reaction of electron-rich phenolate anions with our model system N^5-oxide **1a** leads to rapid, base-mediated dimerization of the flavin with no apparent transfer of oxygen to the phenolates. Dimerization, which occurs via a flavin quinone methide tautomer,[8] is circumvented in the 8-demethylflavin series (e.g., **1b**).[9] Thus, a twofold excess of 8-demethylflavin N^5-oxide **1b** reacts upon mixing in the dark (ambient temperature, anaerobic conditions in tetrahydrofuran) with phenolate **3a** or **3b**. The UV absorption associated with N^5-oxide **1b** (λ_{max} 460 nm) decays with the appearance of absorption due to flavin **6** (λ_{max} 440 nm). Gas–liquid chromatography (GLC) immediately after mixing shows duroquinone (**8a**) formed from phenolate **3a** plus N^5-oxide **1b**, and benzoquinone **8b** and dimer **9** formed from phenolate **3b** plus N^5-oxide **1b** (see Table I). Structure assignments follow from GLC coinjection[10] and comparison of GLC/mass spectral fragmentation patterns to those of authentic samples[10] and, in the case of duroquinone (**8a**), from isolation of the oxidized substrate from the reaction mixture.

Transfer of the N^5-oxide oxygen atom to the phenolates is rigorously established by synthesis and reaction of N^5-[^{18}O-*flavin*]oxide **1c**. As shown in Table I the transfer of isotopic label (^{18}O) from **1c** to phenolate **3a** is virtually quantitative. A

Table I. Products from Flavin N^5-Oxides and Sodium Phenolates

reactants	products, % yield
1b/**3a**	**8a**, 9%[a,b] 2,3,5,6-tetramethylphenol, 26%[a] **6**, 44% isolated (TLC)
1c (28.1% ^{18}O label)[c]/**3a**	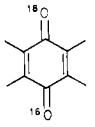 (27.9% ^{18}O label)[b,c]
1b/**3b**	**8b**, 38%[a] **9**, 25%[a] 2,6-di-*tert*-butylphenol, 12%[a]

[a] GLC yield vs. internal standard. [b] A second product ($C_{10}H_{14}O_2$, GLC/mass spectrum) is formed in the reaction of **1b**/**3a**; the product derived from **1c**/**3a** shows 30.5% ^{18}O label (mass spectrum, *m/e* 166 and 168). Isolation attempts (LC, GLC, high vacuum transfer) have proven unsuccessful; silylation of the material derived from **1c**/**3a** with trimethylsilyl chloride/pyridine yields a substance ($C_{13}H_{22}SiO_2$, GLC/mass spectrum) with 26.6% ^{18}O label (mass spectrum, *m/e* 238 and 240). [c] Isotopic abundance determined by mass spectrometry.

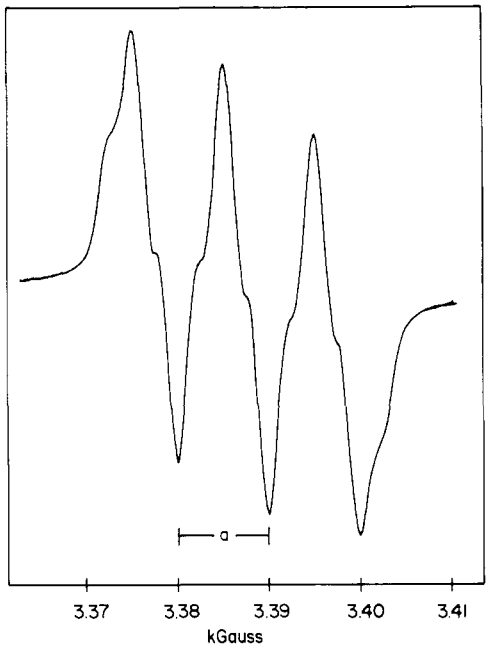

Figure 1. ESR spectrum obtained upon mixing flavin N^5-oxide **1b** and phenolate **3b**. The hyperfine splitting (a = 9.94 G) and triplet character of the absorption are indicative of a nitroxyl radical (see **2b**, Scheme I). Conditions of ESR spectroscopy: microwave frequency, 9.56 GHz; microwave power, 1 mW; modulation amplitude, 0.5 G; modulation frequency, 100 kHz; magnetic field sweep rate, 25 G/min; time constant, 0.1 s; sample temperature, ambient.

(8) Frost, J. W.; Rastetter, W. H. *J. Am. Chem. Soc.* **1980**, *102*, 7157.

(9) (a) For the synthesis of **1b** and **1c** see the general procedures cited in our earlier paper.[7] (b) data for **1b**: ^{1}H NMR (60 MHz, $CDCl_3$) δ (Me_4Si) 0.7–1.4 (m, 24 H), 2.0–3.0 (m, 4 H), 2.5 (s, 3 H), 3.4 (s, 3 H), 4.0–5.8 (m, 7 H), 7.6 (s, 2 H), 8.2 (s, 1 H); ^{13}C NMR (22.6 MHz, $CDCl_3$) δ (Me_4Si) 176.3, 175.8, 175.6, 175.2, 156.0, 153.9, 151.1, 136.7 (2 lines), 134.4, 131.9, 124.4, 121.0, 116.2, 69.9, 68.9, 61.5, 43.9, 33.6 (multiple lines), 27.9, 20.7, 18.6 (multiple lines); IR(KBr) 2970, 2930, 2870, 1730, 1700, 1650, 1585, 1540, 1450, 1400, 1380, 1350, 1270, 1240, 1180, 1135, 1060, 920, 845, 805, 780, 750, 600, 455, 410 cm^{-1}; UV ($CHCl_3$) λ_{max} 485 shoulder (ϵ 5.3 × 10^3), 460 (ϵ 6.6 × 10^3), 440 (ϵ 5.5 × 10^3), 360 shoulder (ϵ 7.1 × 10^3), 345 (ϵ 9.4 × 10^3), 330 shoulder (ϵ 7.9 × 10^3), 270 nm (ϵ 2.9 × 10^4); field-desorption MS, *m/e* 672 (M^+). Anal. Calcd for $C_{33}H_{44}N_4O_{11}$: C, 58.91; H, 6.61; N, 8.33. Found: C, 58.91; H, 6.66; N, 8.05. (c) Field-desorption mass spectrum for **1c**, *m/e* 672, 674 (M^+, ^{16}O, and ^{18}O). (d) The blocking N^3-methyl group of **1b**,**c** prevents proton transfer from the imide N–H (see **1a**) to the phenolates.

(10) SE-30, 4.1% on Chromosorb G, 7 ft × 1/8 in.; GLC/mass spectral comparisons done on SE-30 and OV-17 columns.

Scheme II

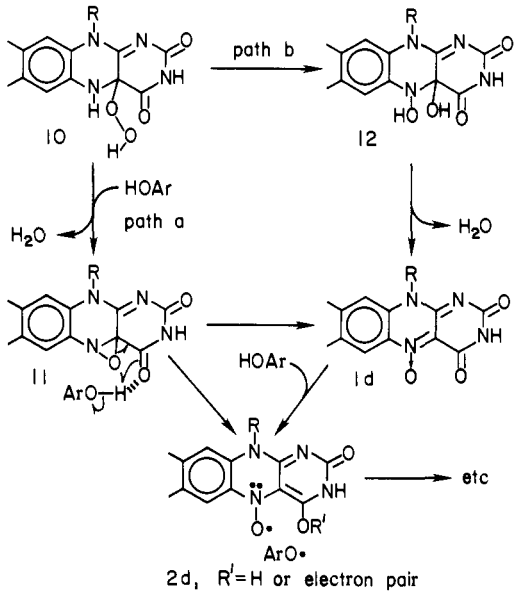

mechanism (Scheme I) consistent with the observed oxygen transfer is initiated by electron transfer from phenolate to flavin N^5-oxide (**1b** + **3a,b** →**2b**/**4a,b**) followed by coupling (**2b**/**4a,b** → **5**) and fragmentation **5** → **6** + **7a,b**). Oxidation of hydroxylated products **7a,b** by the second equivalent of N^5-oxide **1b**[7] affords benzoquinones **8a,b**. The suggested scheme is precedented by phenolic oxidations effected by Fremy's salt[11a] and other, isolable nitroxyl radicals.[11b]

A flavin nitroxyl radical is central to our mechanistic interpretation of the photochemical (see **2a**) and thermal (see **2b**) oxygen transfer from flavin N^5-oxides. The formation of phenol dimer **9** from the reaction of phenolate **3b** with N^5-oxide **1b** suggests that a substantial amount of nitroxyl radical **2b** diffuses out of the solvent cage surrounding **2b**/**4b** prior to the coupling reaction (**2b**/**4b** → **5**). Mixing of **1b** and **3b** in the dark (ambient temperature, anaerobic conditions in tetrahydrofuran) in an ESR cavity results immediately in a strong ESR signal (Figure 1). The three line pattern centered at $g = 2.0163$ ($a = 9.94$ G) is clearly indicative of a nitroxyl radical (see **2b**). Computer simulation of the coupling from N^5, N^{10}, and the protons at C^6 and C^8, along with the assumption of no spin density in the pyrimidine ring[12] of **2b**, affords a simulated spectrum closely approximating the observed signal.[13] On the basis of the hyperfine splitting, the spin density at N^5 is calculated to be $\rho = 0.35$–0.53, indicating stronger localization of the odd electron at N^5 than observed for the neutral flavin semiquinone or flavin semiquinone anion.[14]

Our model system demonstrates the facile thermal generation of a flavin N^5-nitroxyl radical and implicates the radical in the hydroxylation of phenols. On the basis of these results, a flavin N^5-nitroxyl radical is a viable candidate for the ultimate hydroxylating agent in the flavoprotein monooxygenases. Also, in vivo oxygen transfer from N^5 of the coenzyme to phenolic substrates is consistent with the known geometry of the active site of *p*-hydroxybenzoate hydroxylase.[15] A complete description of the flavoprotein monooxygenation of phenols, however, must also include details for the conversion of the putative 4α-(hydroperoxy)flavin **10** (Scheme II) into the N^5-nitroxyl radical. The conversion requires an N–O bond-forming step at N^5 of the coenzyme. Two paths can be envisaged for this step differing in which oxygen atom of the 4α-hydroperoxide **10** becomes attached to N^5 and ultimately is transferred to the phenol (Scheme II).

Dehydration of **10** (path a) would generate the Dolphin–Orf oxaziridine **11**;[16] rearrangement of **10** (path b) would afford hydroxylamine **12**. Chemical precedent and a consideration of bond energies suggest that both paths a and b are exothermic.[17] The dehydration **10** → **11** of path a is directly precedented by the conversion of other α-hydroperoxyamines into oxaziridines.[18] Also, for path a the nucleophile, N^5, is ideally situated for the presumably favored collinear backside displacement (cf. S_N2) by nitrogen on the O–O bond.[19] For path b the attack of N^5 at the distal oxygen atom is precedented, at least intermolecularly, by both enzymatic[3b] and model[4] oxidations of secondary amines by flavin 4α-hydroperoxides. The more exothermic[17] path b, nonetheless, may be geometrically disfavored by the constraints imposed by the attack of N^5 at the distal oxygen atom.[19]

Active site decomposition of hydroperoxide **10** along either path a or b could lead ultimately to the flavin N^5-nitroxyl radical. We have proposed previously[7] a substrate-induced homolysis of oxaziridine **11** leading directly to the mutually reactive (vide supra) pair **2d**/ArO·.[20] The present model study provides support for the proposed coupling of **2d**/ArO· but does not address the prior, phenol-induced homolytic step. Alternatively, flavin N^5-oxide **1d**, formed by rearrangement of **11**[21] or dehydration of **12**, could serve as in vivo precursor to the flavin nitroxyl radical **2d**.[20] Electron transfer from substrate to flavin N^5-oxide (cf. **1b** + **3a,b** → **2b** + **4a,b**, Scheme I) could be induced by partial or complete enzyme deprotonation of the phenol. The binding of the N^5-oxide to the apoprotein might also facilitate electron transfer from the phenolic substrate by perturbing the *N*-oxide reduction potential to a more positive value.[22,23]

A number of flavin-bound oxidants have been proposed to explain flavoprotein monooxygenations.[24] Recent, elegant model studies[4,5] have focused on the delivery of oxygen from the 4α position of the flavin to the substrate. The present work, at the minimum, suggests that transfer of oxygen from the flavin N^5 nitrogen to phenolic substrates must also be considered. Specifically, the in vivo ortho hydroxylation of phenols by flavoprotein monooxygenases is consistent with the generation and coupling

(11) (a) Teuber, H.-J.; Dietz, K. H. *Angew. Chem., Int. Ed. Engl.* **1965**, *4*, 871. (b) Forrester, A. R.; Thompson, R. H. *J. Chem. Soc. C* **1965**, 1224; **1966**, 1844.

(12) This is in accord with the spin density distributions in the neutral flavin semiquinone and flavin semiquinone anion; see ref 14.

(13) A complete hyperfine coupling scheme for the flavin nitroxyl radical must await the synthesis and generation of isotopically substituted (e.g., ^{15}N and ^2H) nitroxyl radicals.

(14) (a) Ehrenberg, A.; Müller, F.; Hemmerich, P. *Eur. J. Biochem.* **1967**, *2*, 286. (b) Müller, F.; Hemmerich, P.; Ehrenberg, A.; Palmer, G.; Massey, V. *Ibid.* **1970**, *14*, 185.

(15) Wierenga, R. K.; de Jong, R. J.; Kalk, K. H.; Hol, W. A. J.; Drenth, J. *J. Mol. Biol.* **1979**, *131*, 55.

(16) Orf, H. W.; Dolphin, D. *Proc. Natl. Acad. Sci. U.S.A.* **1974**, *71*, 2646.

(17) Both paths entail the breaking of O–O and N–H bonds and the formation of N–O and O–H bonds (net downhill by ca. 36 kcal/mol). A correction for oxaziridine ring strain will make path a less exothermic.

(18) (a) Höft, E.; Rieche, A. *Angew. Chem., Int. Ed. Engl.* **1965**, *4*, 524. (b) Schulz, M.; Rieche, A.; Becker, D. *Chem. Ber.* **1966**, *99*, 3233. (c) Hawkins, E. G. E. *J. Chem. Soc. C* **1969**, 2686. (d) *Angew. Chem., Int. Ed. Engl.* **1973**, *12*, 783.

(19) See discussion and references cited by: Sharpless, K. B.; Verhoeven, T. R. *Aldrichim. Acta* **1979**, *12*, 63.

(20) Using the technique of rapid-freeze ESR, Massey and co-workers were unable to detect radical species during the reoxidation of the reduced *p*-hydroxybenzoate hydroxylase–substrate complex by molecular oxygen. See Howell, L. G.; Massey, V.; Strickland, S. *Wenner-Gren Cent. Int. Symp. Ser.* **1972**, *18*, 445. The rapid-freeze technique will stop second-order reactions which rely on diffusion to bring reactive species together in solution; rapid freezing may be of no avail in preventing reaction of closely bound species **2d**/ArO· (see: Ballou, D. P.; Palmer, G. A. *Anal. Chem.* **1974**, *46*, 1248).

(21) The thermal rearrangement of *N*-aryloxaziridines to nitrones is well-known. See: Paquett, L. A. "Principles of Modern Heterocyclic Chemistry"; W. A. Benjamin: New York, 1968; p 70.

(22) Tighter binding of the radical anion **2d** as compared to *N*(5)-oxide **1d** would facilitate electron transfer. Similar effects are seen with the FAD/$FADH_2$ couple.[2a]

(23) Massey et al., using stop-flow techniques, have demonstrated the intermediacy of at least two species, in addition to the putative 4α-hydroperoxide, during flavin cofactored hydroxylation of 2,4-dihydroxybenzoate and other activated aromatics. Massey's third intermediate is suggested to be the 4α-hydroxyflavin based on the absorption maximum (λ_{max} 380–385 nm) of the species.[3d,24] Our mechanism does not include the intermediacy of the 4α-hydroxyflavin; yet it may be possible to account for all of the observed intermediates with our Scheme II or a tautomeric equivalent. It is difficult, however, to judge the lifetime and spectral characteristics of all of our proposed intermediates. See also discussion in ref 5a.

(24) Recent review: Bruice, T. C. *Acc. Chem. Res.* **1980**, *13*, 256.

of the radical pair **2d**/ArO· (Scheme II). A search for further support of the nitroxyl radical flavoenzyme mechanism remains for future investigation.

Acknowledgment. We thank Professor William Orme-Johnson for advice and assistance with ESR spectroscopy and Dr. C. Costello and E. Block for mass spectra. We also acknowledge Professors C. Walsh and T. C. Bruice and Dr. R. Spencer for their interest and insightful discussions. This work was funded by the National Institutes of Health (Grant CA20574) and the Alfred P. Sloan Foundation.

Laser Synthesis of Metal Clusters from Metal Carbonyl Microcrystals

M. A. Duncan, T. G. Dietz, and R. E. Smalley*

Rice Quantum Institute and Department of Chemistry
Rice University, Houston, Texas 77001

Received May 11, 1981

While investigating the photoionization behavior of iron pentacarbonyl in a supersonic beam, we have recently come across evidence for a novel laser photolytic process whereby microcrystals of $Fe(CO)_5$ are efficiently converted in a single laser shot into Fe_x clusters (x = 1–30). This process is remarkable in that it involves (1) wholesale reorganization of the chemical arrangement within a van der Waals bound molecular crystallite prior to vaporization of this crystal and (2) laser excitation in a restricted region of what appears to be an entirely diffuse absorption spectrum. Although the results reported below refer only to ultracold microcrystals of iron pentacarbonyl traveling collision-free at supersonic velocity in a molecular beam, this laser-induced reorganization to Fe_x should also occur within the first 100 Å of the surface of a bulk phase $Fe(CO)_5$ crystal. Since sublimable carbonyl species are readily available for most of the transition metals, this laser chemistry may offer quite interesting new possibilities for polynuclear metal cluster synthesis on a macroscopic scale.

One of the oldest preparative techniques for multinuclear metal clusters is simply irradiation by direct sunlight.[1] In fact this remains a favored technique for the synthesis of $Fe_2(CO)_9$ and very recently has been used to produce new cluster species such as $(\eta^5\text{-}C_5H_5)Nb_3(CO)_7$.[2] In the case of $Fe(CO)_5$, the primary photochemical event in condensed phases is believed to be ejection of CO to form $Fe(CO)_4$[3,4] which is then free to participate in further reactions such as cluster formation.

$$Fe(CO)_4 + Fe(CO)_5 \rightarrow Fe_2(CO)_9$$

Addition of more $Fe(CO)_4$ radicals to produce larger clusters is known to occur, but only when the reaction mixture is heated and then only in small yield. Under normal photolytic conditions the dimer concentration is limited by the fact that metal–metal bond scission is likely the favored primary process.[5] Prolonged exposure to light will ultimately lead to the decomposition of $Fe(CO)_5$ to produce bulk metallic iron and CO gas; so it is clear that some mechanisms do exist for the photolytic production of larger clusters. Under conventional conditions, however, these mechanisms are slow and never result in a substantial yield of metal clusters of intermediate size. The following experiment indicates that a much more favorable situation exists under intense pulsed ArF excimer laser irradiation.

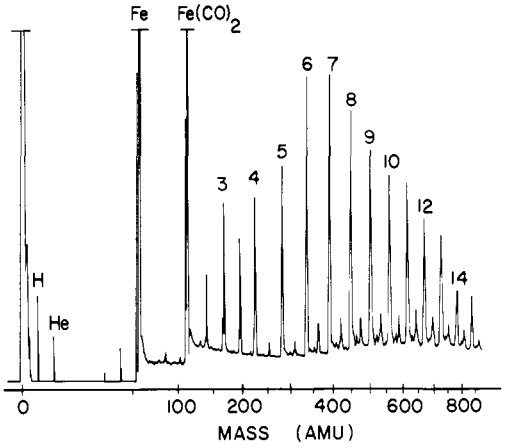

Figure 1. Time-of-flight mass spectrum of ions produced by ArF laser excitation of a $Fe(CO)_5$ microcrystal beam. Numbered peaks are predominantly due to bare iron clusters. Partially fragmented clusters of the type $Fe_x(CO)_y$ where y is odd are seen as small peaks between the larger numbered features. Although these large peaks must contain some contribution from the even y clusters, there is no reason to expect a dominance of these even species in the partially fragmented distribution.

A metal carbonyl microcrystal beam was produced by pulsed supersonic expansion of 0.2% $Fe(CO)_5$ in 15 atm of helium from a 0.1-cm diameter orifice at 300 K. The supersonic nozzle used in this work has been described previously.[6] After careful collimation and differential pumping, the resultant beam passed through a time-of-flight photoionization mass spectrometer[7] where various lasers were used to photolyze and interrogate the content of the molecular beam. Using an excimer laser operating on the F_2 transition at 1570 Å, the presence of iron pentacarbonyl microcrystals was readily monitored since all crystals larger than $[Fe(CO)_5]_3$ are directly photoionized at this wavelength to produce primarily ions of the type $[Fe(CO)_5]_n^+$. However, as shown in Figure 1, drastically different results are observed when the excimer laser is operated on the ArF transition at 1930 Å. The strong mass peaks corresponding to Fe and $Fe(CO)_2$ shown off scale in this figure are due to multiphoton ionization of $Fe(CO)_5$ monomer in the beam.[8] The strong mass peaks numbered from 3 to 14 arise from ArF laser photolysis of the $[Fe(CO)_5]_n$ microcrystals and occur in the appropriate mass channels for the bare clusters Fe_3 through Fe_{14}. The apparent cluster distribution shown in the figure is distorted by the fact that only one mass is perfectly focused onto the detector at any one time. Mass spectra optimized for larger clusters show the distribution to extend with good intensity out to approximately Fe_{30}.

Generation of these Fe_x clusters was found to be strongly dependent on ArF laser fluence. Halving this fluence from 20 to 10 mJ cm^{-2} reduced the Fe_x cluster intensity by a factor of 20. Excitation with the 4th harmonic of a Nd:YAG laser at 2650 Å failed to produce any significant cluster photoion signal other than the very strong Fe and very weak FeCO and $Fe(CO)_2$ signals expected from $Fe(CO)_5$ monomer.[8] This remained true for all laser fluences from 0–100 mJ cm^{-2} (4-ns pulse). Even though the absorption cross section for $Fe(CO)_5$ at 2650 Å is only about one-half of that at 1930 Å,[4] the fluence range explored with the 2650-Å laser was more than sufficient to achieve equivalent energy deposition.

At 20 mJ cm^{-2}, a 10-ns ArF laser pulse will excite $Fe(CO)_5$ molecules at a rate of roughly 2×10^8 s^{-1}. Microcrystals of less

(1) Speyer, E.; Wolf, H. *Ber. Dtsch. Chem. Ges.* **1927**, *60*, 1424–1425.
(2) Herrmann, W. A.; Biersach, H.; Ziegler, M. L.; Weidenhammer, K.; Siegel, R.; Rehder, D. *J. Am. Chem. Soc.* **1981**, *103*, 1692–1699.
(3) For a review of metal carbonyl photochemistry, see: Wrighton, M. *Chem. Rev.* **1974**, *74*, 401–430.
(4) (a) Nathanson, G.; Gitlin, B.; Rosan, A. M.; Yardley, J. T. *J. Chem. Phys.* **1981**, *74*, 361–369. (b) Yardley, J. T.; Gitlin, B.; Nathanson, G.; Rosan, A. M. *Ibid.* **1981**, *74*, 370–378.
(5) Wrighton, M. S.; Ginley, D. S. *J. Am. Chem. Soc.* **1975**, *97*, 2065–2072.
(6) Liverman, M. G.; Beck, S. M.; Monts, D. L.; Smalley, R. E. *J. Chem. Phys.* **1979**, *70*, 192–198.
(7) Dietz, T. G.; Duncan, M. A.; Liverman, M. G.; Smalley, R. E. *J. Chem. Phys.* **1980**, *73*, 4816–4821.
(8) Duncan, M. A.; Dietz, T. G.; Smalley, R. E. *Chem. Phys.* **1979**, *44*, 415–419.

0002-7863/81/1503-5245$01.25/0